Science of the Total Environment 848 (2022) 157628

Contents lists available at ScienceDirect

Science of the Total Environment

journal homepage: www.elsevier.com/locate/scitotenv

New insights into modeling two-step nitrification in activated sludge systems – The effects of initial biomass concentrations, comammox and heterotrophic activities

Mohamad-Javad Mehrani [a], Dominika Sobotka [a], Przemyslaw Kowal [a], Jianhua Guo [b], Jacek Mąkinia [a,*]

[a] Faculty of Civil and Environmental Engineering, Gdansk University of Technology, Narutowicza Street 11/12, 80-233 Gdansk, Poland
[b] Australian Centre for Water and Environmental Biotechnology (ACWEB, formerly AWMC), The University of Queensland, St. Lucia, Queensland 4072, Australia

HIGHLIGHTS

- Two-step nitrification model was expanded with comammox and heterotrophic activity.
- The model was evaluated against data from long-term washout experiments in an SBR.
- The model accurately predicted behavior of N species and microbial relationships.
- The initial biomass concentrations strongly influenced model predictions over time.
- Denitrifying heterotrophs grew only on SMP but remained the dominant microbial group.

GRAPHICAL ABSTRACT

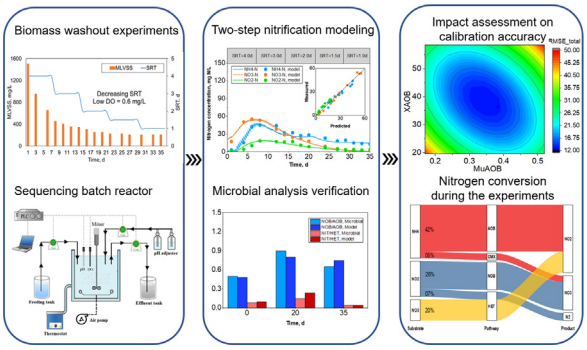

ARTICLE INFO

Editor: Qilin Wang

Keywords:
Process simulation
Complete ammonia oxidation (comammox)
Ammonia-oxidizing bacteria (AOB)
Nitrite-oxidizing bacteria (NOB)
Response surface methodology (RSM)
Two-step nitrification

ABSTRACT

In this study, the conventional two-step nitrification model was extended with complete ammonia oxidation (comammox) and heterotrophic denitrification on soluble microbial products. The data for model calibration/validation were collected at four long-term washout experiments when the solid retention time (SRT) and hydraulic retention time (HRT) were progressively reduced from 4 d to 1 d, with mixed liquor suspended solids (MLSS) of approximately 2000 mg/L at the start of each trial. A new calibration protocol was proposed by including a systematic calculation of the initial biomass concentrations and microbial relationships as the calibration targets. Moreover, the impact assessment of initial biomass concentrations (X) and maximum growth rates (μ) for ammonia-oxidizing bacteria (AOB), nitrite-oxidizing bacteria (NOB), comammox *Nitrospira*, and heterotrophs on the calibration accuracy were investigated using the response surface methodology (RSM). The RSM results revealed the strongest interaction of X_{AOB} and μ_{AOB} on the model calibration accuracy. All the examined model efficiency measures confirmed that the extended model was accurately calibrated and validated. The estimated μ values were as follows: μ_{AOB} = 0.38 ± 0.005 d^{-1}, μ_{NOB} = 0.20 ± 0.01 d^{-1}, μ_{CMX} = 0.20 ± 0.01 d^{-1}, μ_{HET} = 1.0 ± 0.03 d^{-1}. For comparison, when using the conventional model, μ_{AOB} and μ_{NOB} increased respectively by 26 and 15 % (μ_{AOB} = 0.48 ± 0.02 d^{-1} and μ_{NOB} = 0.23 ± 0.005 d^{-1}). This study provides better understanding of the effects of the initial biomass composition and the accompanying processes (comammox and heterotrophic denitrification) on modeling two-step nitrification.

* Corresponding author at: Gdansk University of Technology, ul. Narutowicza 11/12, 80-233 Gdansk, Poland.
E-mail address: jmakinia@pg.edu.pl (J. Mąkinia).

http://dx.doi.org/10.1016/j.scitotenv.2022.157628
Received 30 April 2022; Received in revised form 21 July 2022; Accepted 21 July 2022
Available online 26 July 2022

1. Introduction

Nitrification is a key process of nitrogen (N) removal in municipal wastewater treatment plants (WWTPs), consisting of two steps: ammonia oxidation to nitrite (nitritation) followed by nitrite oxidation to nitrate (nitritation). Although nitrification has been known since the end of the 19th century, the process understanding has changed dramatically in recent 30 years, which was reflected by the evolving descriptions in (Metcalf and Eddy, 2003; Metcalf and Eddy, 2014; Metcalf and Eddy, 1991). The improved understanding of the mechanisms of nitrification has been accompanied with growing attention to nitrite as a central component in the novel autotrophic N removal processes, including deammonification and a shortcut of nitrification-denitrification via nitrite ("nitrite shunt"). As a consequence, the role of nitrite-oxidizing bacteria (NOB) has received the growing attention, but due to the limited knowledge on their metabolism, NOB still remain a "*big unknown of the nitrogen cycle*" (Daims et al., 2016). In particular, the recent discovery of complete ammonia oxidation (comammox) by a single *Nitrospira*-type microorganism (Daims et al., 2015; van Kessel et al., 2015) has overturned "*a century-old dogma of nitrification research*". However, the actual role of comammox-*Nitrospira* in full-scale WWTPs is ambiguous (Koch et al., 2019).

According to r/K theory, the nitrifying bacteria can be divided into r- and K-strategists. The fast-growing r-strategists are represented by ammonia-oxidizing bacteria (AOB) *Nitrosomonas* and NOB *Nitrobacter*, whereas *Nitrospira* is the K-strategist with a high substrate affinity (Yu et al., 2020; Yin et al., 2022). The assumptions of r/K theory are a base for the development of various NOB washout strategies in the novel N removal systems. In general, the controlled solids retention time (SRT), combined with dissolved oxygen (DO)-limited conditions and high residual ammonia, have been identified as the most common NOB wash-out strategies (Regmi et al., 2014; Gustavsson et al., 2020). However, low DO concentrations (<1.0 mg O_2/L) can be inefficient with respect to the suppression of K-strategist NOB (*Nitrospira)* (Cao et al., 2017). Moreover, low temperature has also been reported as a significant obstacle to NOB suppression (Gilbert et al., 2014; Laureni et al., 2016; Liu et al., 2021).

An efficient approach to investigation of the nitrifier competition under selective pressures would be a combination of dedicated laboratory experiments with mathematical modeling and advanced microbiological analyses. Two-step nitrification models have been known for over 50 years (Knowles et al., 1965), but a simple Monod-type model for ammonia oxidation to nitrate (as a one-step conversion) was sufficient under typical operating conditions of activated sludge systems (Henze et al., 2000). Since the 2000's, with recognizing the central role of nitrite in the novel N removal systems, the interest in two-step models has been growing (see Table S1 in the Supporting Information (SI)).

Very recent advances in modeling two-step nitrification include examination of the competition among the AOB and NOB species for different r/K strategist groups for AOB and NOB (Yu et al., 2020), and incorporation of comammox (Mehrani et al., 2021). However, Yu et al. (2020) ignored heterotrophic (HET) activity and justified that simplification by the fact that the main objective of the study was to investigate the competition among the nitrifiers and the feed contained no organic material. In fact, a significant heterotrophic growth can be observed in autotrophic N systems (fed with no organic carbon), in which the soluble microbial products (SMPs) are the sole organic carbon and energy source for denitrifying heterotrophs (Al-Hazmi et al., 2021). Mozumder et al. (2014) and Liu et al. (2016) developed theoretical models for heterotrophic growth in autotrophic nitrogen removal systems. Lu et al. (2018) adopted that concept to predict high abundances of heterotrophic biomass in a laboratory-scale deammonification system (fed with no organic carbon).

The nitrification models should accommodate appropriately the behavior of AOB and NOB to understand factors influencing the competition between autotrophic N-converting microorganisms (Kaelin et al., 2009; Cao et al., 2017). Therefore, the aim of this study was to revise the traditional approach to modeling two-step nitrification by considering the effect of two accompanying processes (comammox and heterotrophic growth). Furthermore, setting the realistic initial AOB and NOB concentrations and their effects on model predictions were explored as well. This issue, despite critical from a modeling perspective, has not received adequate attention so far (see Table S1). The newly developed model was calibrated and validated based on the results of four long-term washout experiments exploring the effect of temperature at continuously decreasing SRTs. The relative abundances of AOB and NOB were determined by 16S rRNA gene amplicon sequencing followed by phylogenetic analysis. This study contributes to better understanding of the effect of initial biomass composition, as well as the newly discovered comammox and heterotroph activities on model accuracy in the two-step nitrification modeling. Moreover, the contribution of different microorganisms (AOB, NOB, comammox bacteria and heterotrophs) in the N conversion and their population dynamics were predicted.

2. Material and methods

2.1. Design of laboratory experiments and data collection for modeling

2.1.1. Origin of biomass for the laboratory experiments

Fresh samples of mixed liquor (inoculum biomass) were collected twice, in winter (January) and summer (July), from a large WWTP in the town of Swarzewo, which is located in a touristic region on the Baltic Sea coast (northern Poland). The design hydraulic capacity and pollutant load of that plant are 18,100 m^3/d and 177,000 population equivalent, respectively. In the summer months (June–September), the plant treats up to 14,000 m^3/d of wastewater, while the flowrate drops to approximately 5000 m^3/d during the remaining period. In addition to the domestic wastewater, the plant receives a substantial portion (~5 %) of nitrogen-rich wastewater from the fish industry. The biological part of the plant consists of six parallel sequencing batch reactors (SBRs). The effluent quality meets the European Union Urban Wastewater Directive (91/21/EEC) requirements with respect to total N (TN) = 10 mg N/L, total P (TP) = 1 mg P/L, and chemical oxygen demand (COD) = 150 mg COD/L.

2.1.2. Long-term washout experiments

Two 5-week washout experimental series were carried out with the fresh inoculum biomass at the temperatures of 12 °C and 20 °C, close to the actual process temperatures in winter and summer. During each series, the inoculum biomass was diluted to approximately 2000 mg/L with tap water and then poured into two parallel, fully automated plexiglass SBRs (SBR1 and SBR2) with a working volume of 10 L each. The reactors were placed in water coats, coupled with a thermostatic water bath, to keep the selected temperature setpoints. The reactors were equipped with an automated aeration control system which allowed to apply two different aeration modes, i.e. continuous aeration at the DO set point of 0.6 ± 0.1 mg O_2/L (SBR1) v.s. intermittent aeration at 3/9 min on/off periods and the DO set point of 1.2 ± 0.1 mg O_2/L in the "aeration on" period (SBR2). The pH was kept at 7.5 ± 0.2 during all the experiments by automatically dosing NaOH (2 M solution).

The operational conditions in each experiment are summarized in Table 1. One operational cycle lasted 8 h (480 min) and consisted of three phases: feeding (15 min), reaction (aeration) (450 min), and decantation (15 min). The solids retention time (SRT), equal to the hydraulic retention time in an SBR, was aggressively decreasing from the initial 4 d to 1 d

Table 1
Operational parameters and conditions in the reactor during the long-term washout experiments.

Experiment	Temperature (°C)	Aeration mode	DO set-point (mg O_2/ L)	MLSS/MLVSS (mg/L)
T1	12	Continuous	0.6 ± 0.1	1980 / 1450
T2	20	Continuous	0.6 ± 0.1	2146 / 1500
T3	12	Intermittent	1.2 ± 0.1 (3 min on), and 0.0 (9 min off)	2040 / 1600
T4	20	Intermittent	1.2 ± 0.1 (3 min on), and 0.0 (9 min off)	1930 / 1590

at the end of the trial. Each SRT condition (4, 3, 2, 1.5 and 1 d) was kept for one week as shown in Fig. S1 in the SI along with the influent N loading. Table S2 (in the SI) shows the composition of synthetic feed, including the main elements and trace solution.

During the experiments, mixed liquor samples were collected 3 times per week at the beginning and end of the reaction phase. The samples were filtered and analyzed for different forms of nitrogen (NH_4^+-N, NO_3^--N, and NO_2^--N). Mixed liquor suspended solids (MLSS) and mixed liquor volatile suspended solids (MLVSS) were measured at the beginning of the reaction phase. For microbiological analyses, duplicated biomass samples were collected from the reactors three times: at 0 d (beginning), 20 d, and 35 d (end).

2.1.3. Supporting short-term batch experiments

Before each series of the long-term experiments, accompanying batch tests were carried out with mixed liquor from the studied plant. Nitrification rates were measured at different DO concentrations in the range of 0.2–2.5 mg O_2/L at 12 °C (winter series) and 20 °C (summer series). Based on the experimental results, three kinetic parameters ($K_{O,AOB}$, $K_{O,NOB}$, $K_{NO2,NOB}$) were estimated for the two-step nitrification model. The details of those tests and estimation methods can be found in the section S3 (SI).

2.1.4. Chemical and microbiological analysis

Before the analysis, the samples of mixed liquor were filtered under vacuum pressure through a 1.2 μm pore size nitrocellulose filter MFV-3 (Millipore, USA). The analytical procedures, which were adopted by Dr. Lange and Shimadzu, followed the Standard Methods APHA (2002). Concentrations of NH_4^+-N, NO_3^--N, and NO_2^--N were determined using cuvette tests in Xion 500 spectrophotometer (Hach Lange GmbH, Berlin, Germany). The MLSS and MLVSS were determined by the gravimetric method in accordance with the Standard Methods APHA (2002).

The biomass samples withdrawn for microbiological analyses were stored at −25 °C. Deoxyribonucleic acid (DNA) extraction from the thawed samples was performed with FastDNA™ SPIN KIT (MP Biomedicals, USA) following the manufacturer's manual. The genomic DNA extracts from the duplicated samples were pooled together. The DNA acquired from purification was subsequently used for the Illumina Next Generation Sequencing protocol. High-throughput Illumina sequencing the V3-V4 regions of the 16S rRNA gene protocol and following DNA sequencing data processing and analysis were carried out as described in our previous studies (Al-Hazmi et al., 2021). The dynamics of the comammox bacteria population were monitored by the quantitative polymerase chain reaction (qPCR) with two sets of primers comaA-244F and coma-659 R, and comaB-244F and comaB-659R, both targeting *amoA* gene encoding ammonium monooxygenase specified for comammox *Nitrospira* as proposed by Pjevac et al. (2017). The qPCR protocol is presented in detail in the SI file.

2.2. Organization of the modeling study

The entire modeling study was organized in six steps as shown in Fig. 1. Each step was described in the following sub-sections.

2.2.1. Mathematical model development and implementation

The GPS-X software 8.0 (Hydromantis, Canada) was used as a modeling and simulation tool. The Activated Sludge Model No. 1 (ASM1) (Henze et al., 2000), incorporating a one-stage nitrification process, was expanded with two-step nitrification and comammox (Mehrani et al., 2021). The two-step denitrification equations were adopted from Mantis2 model (Hydromantis).

In comparison with the conventional two-step nitrification model (Fig. 2A), the newly developed model incorporated comammox and heterotrophic denitrification on SMP in the nitrogen conversions (Fig. 2B). Comammox was modeled as a one-step process (NH_4^+-N → NO_3^--N). It was assumed that comammox bacteria are not able to utilize NO_2^--N as an electron donor based on the observed disappearing comammox activity in an experiment with NO_2^--N as a sole substrate (data not shown). In literature, Koch et al. (2019) explained this disability of comammox *Nitrospira* by the lack of assimilatory nitrite reductase.

2.2.2. Setting the initial biomass composition

For dynamic simulations, the ASM-type models require setting the initial concentrations of specific groups of microorganisms. In this study, mass balance calculations were combined with the results of microbiological analyses. The entire procedure consisted of three steps as shown in Fig. S3 in the SI. In the first step, nitrifier concentrations were calculated based on the mass balance equations (Metcalf and Eddy, 2014). Both operational parameters (flowrate, reactor volume, SRT and load of nitrified nitrogen) and kinetic/stoichiometric coefficients (specific decay rates, yields) were used as input data. Next, AOB, NOB, comammox and heterotrophic biomass concentrations were estimated as relative abundances in the general microbial community, based on the data obtained from the high-throughput 16S rRNA gene amplicon sequencing and qPCR. It was assumed that heterotrophic microorganisms that decreased their share over time were treated as slowly biodegradable substrate (X_S). Finally, the concentration of particulate inert organic compounds (X_I) was determined by subtracting the other organic fractions from MLVSS.

2.2.3. Sensitivity analysis and correlation matrix

The initial steps comprised sensitivity analysis (SA) and the development of a correlation matrix, to reduce the number of model parameters adjusted during calibration. Altogether, 13 kinetic coefficients that target N components, including NH_4^+-N, NO_2^--N, and NO_3^--N, were considered. A special GPS-X sensitivity analyzer utility was used to run simulations under the uncertainty of 20 % (10 % of the adjusted value) for each parameter as described by Lu et al. (2018).

The sensitivity analysis was followed by building the correlation matrix (C_θ) based on the variance-covariance matrix (Eq. (1)):

$$(C_\theta)_{k,l} = \frac{(V_\theta)_{k.l}}{\sqrt{(V_\theta)_{l.l} \times (V_\theta)_{k.k}}} \quad (1)$$

where (V_θ) is the variance-covariance matrix of the individual parameter estimates (*k*,*k*) and (*l*,*l*), and the different parameter estimates (*k*,*l*).

The correlation matrix evaluates a linear relationship, its strength, and direction (positive vs. negative) of the pairs of influential model parameters. If the determined correlation coefficient is high enough for any pair, the calibration process can be simplified by adjusting only one of the two parameters (Zhu et al., 2015). Cao et al. (2020) classified the correlations values of pair parameters as strong (>0.68), moderate (0.36–0.68) and weak (<0.36), respectively. That classification was adopted in the present study.

2.2.4. Model calibration and validation

Kinetic parameters in the extended model were adjusted based on the T1 experiment data (continuous aeration at 12 °C), whereas the T2 experiment data (continuous aeration at 20 °C) were used for adjusting the temperature correction factors (Table 1). For model calibration, a special GPS-X optimization utility was used and the 95 % confidence intervals were determined for the parameter estimates. The two other experiments (T3 and T4) with intermittent aeration provided data for model validation.

Similar to our previous study (Mehrani et al., 2021), the common performance measures, such as the determination coefficient (R^2), root mean square error (RMSE), and mean absolute error (MAE) were used for evaluation of the model efficiency ("goodness-of-fit"). Moreover, the Janus coefficient (J^2) was determined to compare the model efficiency between the calibration and validation steps (Hauduc et al., 2015).

2.2.5. RSM-based impact assessment of the extended model

The response surface methodology (RSM) assesses the effect of model inputs and their interactions on model outputs while minimizing the number of required simulations (Baruah et al., 2021). In this study, the RSM was applied by Origin 9.8 (OriginLab, USA) to determine the effects of individual and combined interactions of eight important model inputs, including initial biomass concentrations of AOB, NOB, CMX, and HET (X_{AOB}, X_{NOB}, X_{CMX}, X_{HET}) and their maximum growth rates (μ_{AOB}, μ_{NOB}, μ_{CMX}, μ_{HET}), on

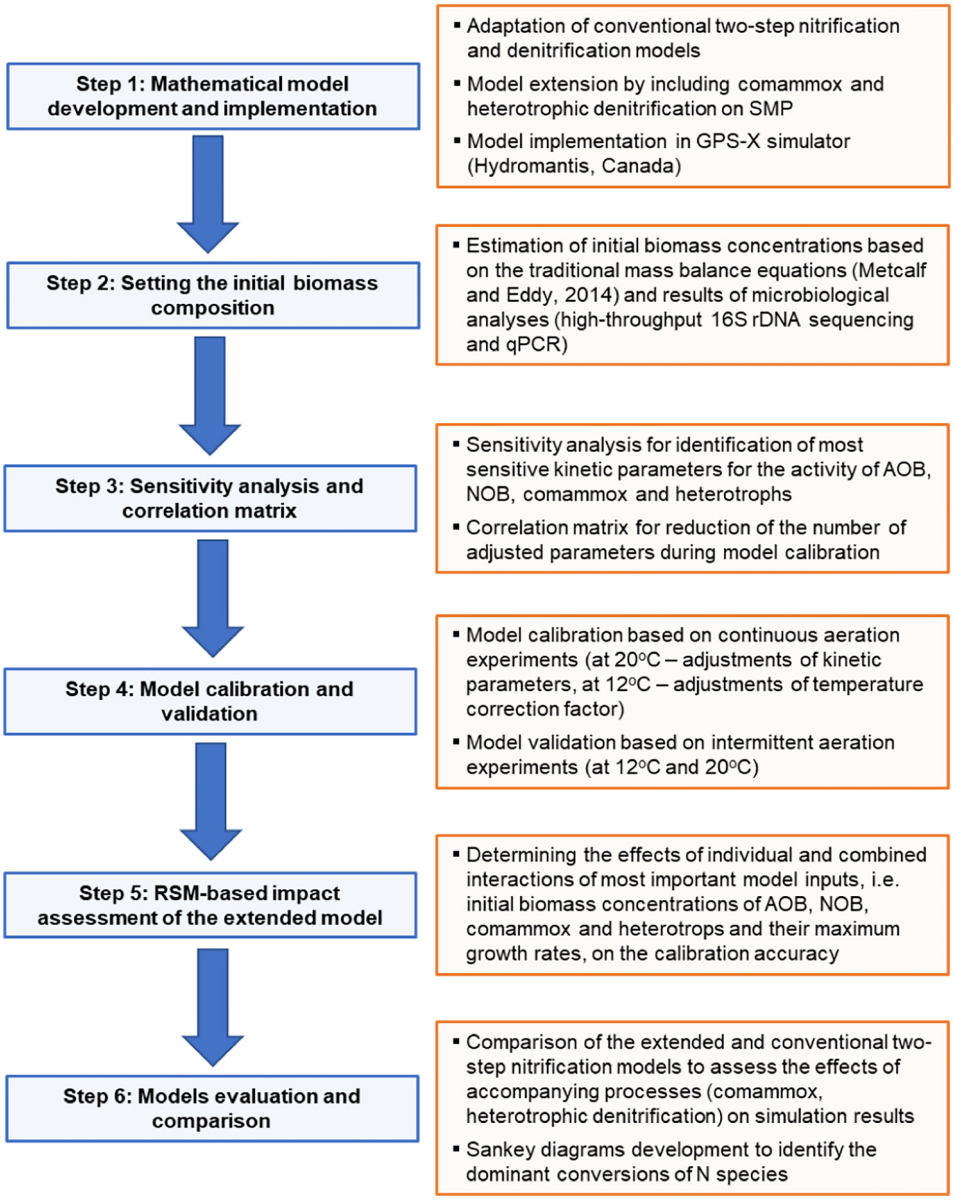

Fig. 1. Flowchart diagram of the modeling procedure and setting of initial biomass concentrations.

the calibration accuracy of the extended model. The RMSE was selected as the accuracy criterion considering the sum of differences between the observed data and model predictions for of N species (NH_4^+-N, NO_3^--N, NO_2^--N) in each simulation.

Initially, the selected model inputs were defined to the RSM. The input model related to the examined experiment T1 were as follows: X_{AOB} = 34.3 mg COD/L, X_{NOB} = 12.5 mg COD/L, X_{CMX} = 6.0 mg COD/L, X_{HET} = 405 mg COD/L, μ_{AOB} = 0.38 d^{-1}, and μ_{NOB} = 0.20 d^{-1}, μ_{CMX} = 0.20 d^{-1}, and μ_{HET} = 1.0 d^{-1}. The range of ±50 % was set to all inputs to evaluate the effects of their individual and combined interactions on the model response (RMSE). Then, the RSM automatically designed the required number of combinations of inputs for simulation with the extended model. All the cases were simulated using GPS-X and the response Y (RMSE) of each case was entered to the RSM.

A mathematical model between the response Y (RMSE) and eight independent inputs x_i/x_j (X_{AOB}, X_{NOB}, X_{CMX}, X_{HET}, μ_{AOB}, μ_{NOB}, μ_{CMX}, μ_{HET}) was described by a second-order polynomial equation (Li et al., 2018) (Eq. (2)):

$$Y = \beta_0 + \Sigma_{i=1}^{n}\beta_i x_i + \Sigma_{i=1}^{n}\beta_{ii}{x_i}^2 + \Sigma\Sigma_{i<j}\beta_{ij}x_i x_j + \epsilon \quad (2)$$

where $\beta_0$is a constant coefficient, β_i are the linear coefficients, β_{ii} are the quadratic coefficients, β_{ij} are the interplay coefficients, x_i and x_j are the coded form of inputs, and ε is the residual error.

The analysis of variance was used to investigate the statistically significant of the model inputs ($p < 0.05$), followed by the importance level (Pareto analysis) to identify the level of significance on the response (RMSE) for input parameter and their interaction (Anupam et al., 2011) (Eq. (3)):

$$P_i = \left(\frac{b_i^2}{\Sigma b_i^2}\right) (i \neq 0) \quad (3)$$

where P_i is the importance level of each single model input or their interaction (b_i). A counter plot was prepared for the coincide effect for the most important pairs of inputs on the response.

2.2.6. Model evaluation and comparison

The extended model was used to evaluate the effect of different bacteria groups (AOB, NOB, comammox and heterotrophs) on the behavior of N

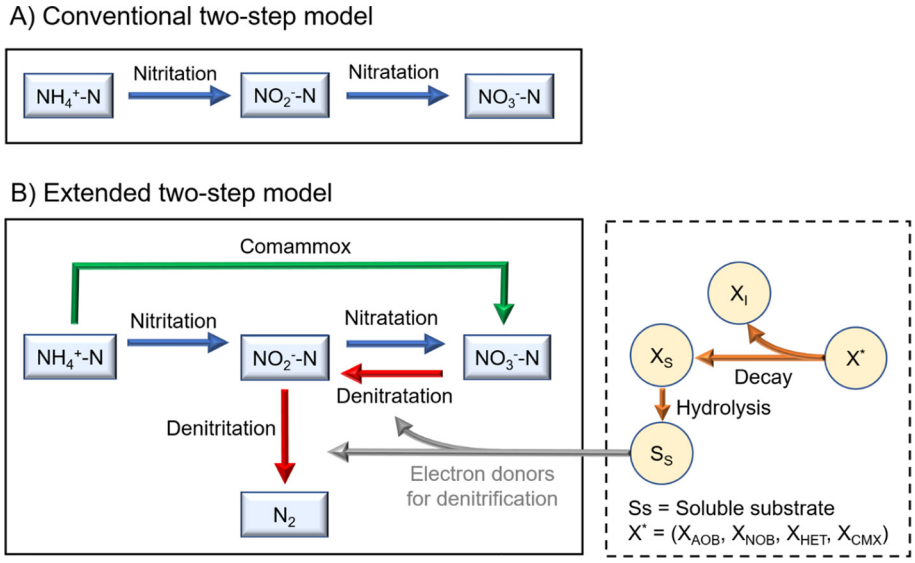

Fig. 2. The conventional (A) and extended model (B) of two-step nitrification.

species (NH_4^+-N, NO_3^--N, NO_2^--N). Based on the predicted conversion rates (mg N/L·d) in experiment T1, the Sankey graphs were developed to identify the dominant N conversions at different stages of the experiment, i.e., at t = 0 d (beginning), t = 20 d and t = 35 d (end). At the same times, the microbial structures were analyzed (see: Section 2.1.2). Moreover, the conventional two-step nitrification model (without considering comammox and heterotrophic activities) was calibrated based on the experiment T1 data. The effect of the accompanying processes (comammox and heterotrophic denitrification) on two-step nitrification was evaluated by comparing the estimated maximum specific growth rates of AOB (μ_{AOB}) and NOB (μ_{NOB}) in the two models (conventional vs. extended) in experiment T1.

3. Results

3.1. Initial biomass concentrations and microbial population dynamics

The calculated initial concentrations of the specific microbial groups (X_{AOB}, X_{NOB}, X_{CMX}, X_{HET}) for experiments T1-T4 can be found in Table S4 (SI). In all the cases, the initial MLSS concentration was approximately 2000 mg/L, and it dropped below 400 mg/L by the end of the experiment. Under the progressive SRT reductions, the populations nitrifiers and heterotrophs revealed substantial changes. The measured NOB/AOB and nitrifier/heterotroph ratios became calibration targets and are further discussed in Section 3.3.

Based on 16S rRNA gene sequencing, the AOB accounted for 2.3 ± 0.1 % of the total bacterial community in the initial samples, whereas the NOB abundance was 1.2 ± 0.2 %, which corresponded to the NOB/AOB ratio of approximately 0.5. The predominant representatives of AOB were bacteria affiliated to the *Nitrosomonas* genera through all the experimental periods, with an average share of 4.3 ± 2.2 % in the total bacterial population during the middle phases of the experiments (SRT ≤ 2.0) and 0.5 ± 0.2 % for the SRT <2.0. The NOB subpopulations were initially composed of *Nitrolancea* (1.0 ± 0.1 %) and *Nitrospira* (0.20 ± 0.05 %), and switched to the predominance of *Nitrospira* in the course of the experiments. While *Nitrolancea* were systematically washed out form the system (the average share in the terminal samples: 0.05 ± 0.01 %), *Nitrospira* raised their contribution in the biomass samples up to 4.8 % for the SRT ≤ 2.0, and reached the averaged share of 0.27 ± 0.11 % at the end. The qPCR data revealed that comammox *Nitrospira* tended to stabilize their shares in the biomass until reaching the shortest SRTs (≤1 d).

Surprisingly, heterotrophic bacteria were the dominant microbial group in all the analyzed samples, even though the influent feed did not contain organic carbon. This could be attributed to the utilization of SMP by heterotrophs (Ni et al., 2011b) (see the discussion in Section 4.3). Monitoring of 20 most abundant heterotrophic taxa revealed the continuously growing shares in the biomass, despite the aggressive washout conditions in the course of the experiments.

3.2. Sensitivity analysis and correlation matrix

Fig. S4 (SI) shows the sensitivity coefficients calculated for all the analyzed kinetic parameters with respect to AOB, NOB, comammox and heterotrophs based on the data from the two experiments (T1 and T2). In experiment T1, the extremely influential ($S_{i,j} \geq 2$) parameters comprised μ of AOB, NOB with respect to the behavior of NO_2^--N, and μ of NOB with respect to the behavior of NO_3^--N. The μ_{AOB} was high influential ($1 \leq S_{i,j} < 2$) for NH_4^+-N concentrations.

The next very influential parameters in experiment T1 were the decay rates (b_{AOB} and b_{NOB}) with Si,j of 1.42–1.98, and DO half-saturation coefficients ($Ko,_{AOB}$ and $Ko,_{NOB}$) with Si,j of 1.3–1.4 for NO_2^--N. All the analyzed parameters for hetrotrophic bacteria were less influential with Si,j < 0.11 and < 0.15 for experiments T1 and T2, respectively. For experiment T2, μ of all nitrifiers were highly influential parameters, followed by the decay rates (b_{AOB} and b_{NOB}) and Ko ($Ko,_{AOB}$ and $Ko,_{NOB}$) related to NO_2^--N and NO_3^--N.

Fig. 3 shows the overall correlation matrix for the most relevant kinetic parameters. In both experiments (T1 and T2), the highest correlation coefficients referred to the link between the maximum growth rates (μ) and decay coefficients (b) for all the nitrifier groups. Furthermore, Ko for all nitrifier groups exhibited a high correlation with the corresponding μ in both experiments.

3.3. Model calibration and validation

Three methods were used to determine the kinetic and stoichiometric parameter values for simulations: (i) literature data, (ii) the direct determination from batch experiments, and (iii) mathematical optimization (parameter estimation). The list of kinetic parameters and their adjusted values are presented in Table 2.

Based on the SA and correlation matrix results (Fig. 3 and Fig. S4), four least influential parameters, including NO_2^--N half-saturation constant for comammox ($K_{NO2,CMX}$), NH_4^+-N half-saturation constants for AOB ($K_{NH4,AOB}$) and comammox ($K_{NH4,CMX}$), and DO half-saturation constant for comammox ($K_{O,CMX}$) were adopted from the literature (Koch et al., 2019; Park et al., 2017; Yu et al., 2020). In addition, three important kinetic parameters, including the NO_2^--N half-saturation constants for NOB ($K_{NO2,NOB}$),

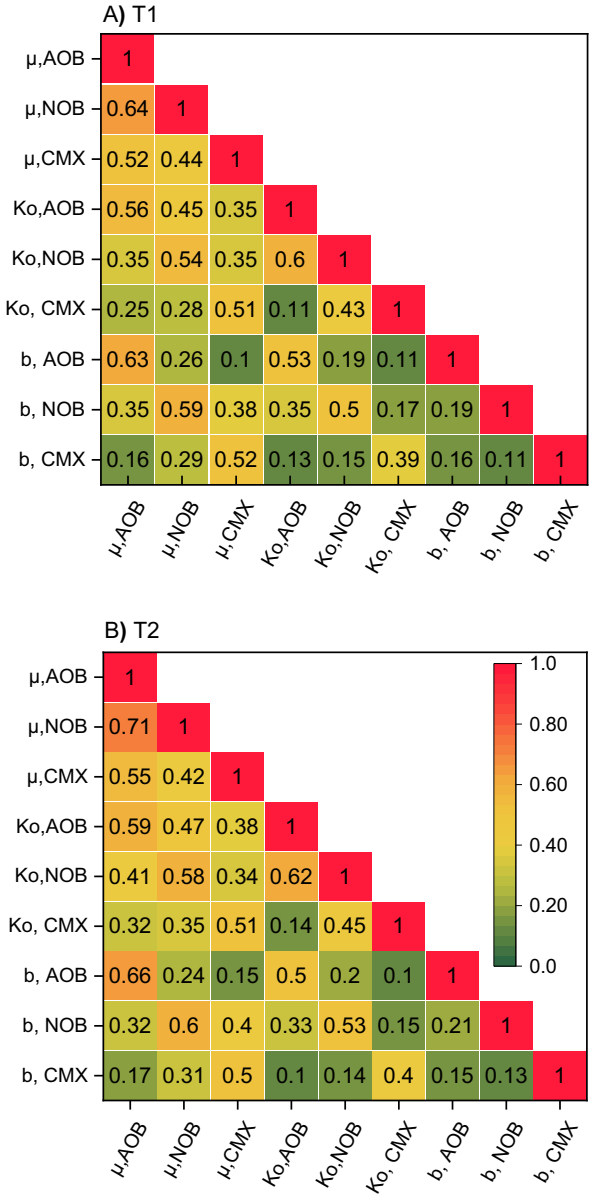

Fig. 3. Correlation matrix for the most sensitive kinetic parameters (μ, Ko, and b), A) experiment T1, B) experiment T2.

and DO half-saturation constants for AOB and NOB ($K_{O,AOB}$, $K_{O,NOB}$), were determined experimentally (Table S2 in the SI). Among four estimation methods, the Hanes equation had the highest determination coefficient ($R^2 > 0.9$) in all the cases.

During parameter estimation with the simplex method, the values of μ and b for all the microbial groups were searched within the ranges reported in literature (Table S5 in the SI). In particular, the low adjusted values of μ, K_O, and K_{NO2} for NOB and comammox *Nitrospira* confirm that these bacteria are typical representatives of the "K-strategists". The values of all optimized parameters fit well the typical ranges reported in literature (Table 2). Only the experimentally determined $K_{O,AOB}$, $K_{O,NOB}$ and $K_{NO2,NOB}$ were approaching the reported low extremes.

The observed and predicted behaviors of N species (NH_4^+-N, NO_3^--N, and NO_2^--N), biomass concentrations and microbial relationships (NOB/AOB and NIT/HET ratios) for the calibrated model are shown in Fig. 4. Similar comparisons for the validated model can be found in the SI (Fig. S5).

In both experiments (T1 and T2) during the calibration phase, the trends of NO_3^--N and NO_2^--N concentrations were generally similar, while the NH_4^+-N behavior was slightly different (Fig. 4a-b). In experiment T1, a small peak (approximately 40 mg N/L) occurred after one week and then the concentration was continuously decreasing and ultimately dropped below 15 mg N/L. On the contrary, in experiment T2, the concentrations increased at the beginning and then stabilized at approximately 25 mg N/L. The NOB/AOB ratios increased from 0.5 to 0.55 at the beginning to 0.9–1.1 at the end of experiment for T1 and 0.8–0.85 for T2. By contrast, the NIT/HET ratios were relatively stable (0.1–0.15) in the first two samples for both T1 and T2, but decreased below 0.1 at the end of experiments (Fig. 4e-f).

Table 3 shows the extended model prediction accuracy independently for each output (NH_4^+-N, NO_3^--N, NO_2^--N). The calibrated model revealed a high goodness-of-fit for all the outputs in terms of R^2 (>0.83) and MAE and RMSE errors (2.17–4.2). When assessing the validated model, R^2 decreased to 0.74–0.85, while the errors (RMSE, MAE) slightly increased (by 10–15 %). The Janus coefficients were in the range of 1.45–2.25 confirming the model validity.

3.4. RSM-based impact assessment of the extended two-step nitrification model

Altogether, 86 combinations of the individual impacts and interactions of eight independent parameters, with ±50 % from their reference values, were designed and evaluated by the RSM. Fig. 5 shows the importance level for all the parameters and their interactions on the response (RMSE for the sum of NH_4^+-N, NO_3^--N, and NO_2^--N). The interaction of X_{AOB} and μ_{AOB} had explicitly the highest importance level of 0.7, followed by the individual effects of μ_{AOB} and μ_{NOB} (importance level > 0.4). In the third ranked importance group (importance level of approximately 0.3), the combined effect of μ_{AOB}*μ_{NOB} was followed by the individual effects of X_{AOB} and μ_{CMX}. The most influential pairs (X_{AOB}*μ_{AOB}, μ_{AOB}*μ_{NOB}, X_{NOB}* μ_{NOB}, μ_{AOB}*μ_{CMX}, μ_{NOB}* μ_{CMX}) with the importance level > 0.2 were selected for showing their simultaneous effect on the response variability (Fig. 6).

3.5. Contribution of accompanying processes in N conversions

The Sankey graphs (Fig. 7) were developed based on the predicted process rates to assess the nitrogen conversion pathways at $t = 0$ d (beginning), 20 d, and 35 d (end). In the course of the experiment, the relative contributions of each specific bacteria group were subjected to significant rearrangements. A continuous decreasing trend was observed with respect to the canonical NOB (from 39 to 13 %) and comammox bacteria (from 18 % to 2 %). In contrast, the contribution of denitrifying heterotrophs, performing two steps of denitrification, was increasing from the initial 6.5 % to 68.5 % at the end. The contribution of AOB was 35 % at the beginning and decreased to 16 % at the end, after rising to 49 % in the middle phase.

3.6. Comparison of the conventional and extended two-step nitrification model

In comparison with the extended model, the accuracy of the conventional model predictions did not change considerably, but the estimates of the maximum specific growth rates for AOB and NOB were different in both models. When all the other kinetic parameters for AOB and NOB were assumed the same as in the extended model (Table 2), the μ values for AOB and NOB increased by 26 and 15 %, respectively, i.e., $\mu_{AOB} = 0.48 \pm 0.02\ d^{-1}$ and $\mu_{NOB} = 0.23 \pm 0.005\ d^{-1}$. Furthermore, the model efficiency of the conventional model was slightly worsened for all the N species, which was reflected by lower R^2 values (0.86–0.91) and MAE and RMSE (2.5–5.1).

4. Discussion

4.1. Initial concentrations of AOB and NOB

The results of RSM revealed the importance of the initial biomass concentrations for accurate simulation of the dynamic behavior of all N species. Surprisingly, that issue has not received attention in the previous

Table 2
List of the kinetic and stoichiometric parameters used for simulations, including the parameters optimized and estimated in laboratory experiments.

Parameter	Unit	Bacterial group				Basis for estimation
		AOB	NOB	CMX	HET	
Kinetic						
μ	d^{-1}	0.38 ± 0.005 (0.2–0.9)[g]	0.2 ± 0.01 (0.18–0.9)[g]	0.2 ± 0.01 (0.15–0.22)[h]	1.0 ± 0.03 (0.5–6.0)[k]	Optimization
K_O	mg O_2/L	0.17	0.13	0.33[a]	0.2[e]	Batch test/Literature
K_{NH4}	mg NH_4/L	0.67[b]	–	0.012[c]	–	Literature
K_{NO2}	mg NO_2/L	–	0.06	–	0.2[e]	Batch test / Literature
K_{NO3}	mg NO_2/L	–	–	–	0.2[e]	Literature
b	d^{-1}	0.15 ± 0.004 (0.05–0.15)[i]	0.04 ± 0.006 (0.03–0.05)[i]	0.04 ± 0.006 -	0.4 ± 0.02 (0.2–0.62)[l]	Optimization
Stoichiometric						
Y	gCOD/gN	0.15[d]	0.05[d]	0.15[f]	–	Literature
Y	gCOD/gCOD	–	–	–	0.6[e]	Literature
Correction factor, θ						
for μ	–	1.09[j]	1.11[j]	1.09[f]	1.03[j]	Literature
for b	–	1.029[j]	1.029[j]	1.029[f]	1.029[j]	Literature

μ: Max. specific growth rate, K_O: DO half-saturation constant, K_{NH4}: Ammonia half-saturation constant, K_{NO2}: Nitrite half-saturation constant, Y: Yield coefficient, b: Decay rate, θ: Temperature correction factor.
[a] (Park et al., 2017).
[b] (Yu et al., 2020).
[c] (Koch et al., 2019).
[d] (Metcalf and Eddy, 2003).
[e] (Hiatt and Grady, 2008).
[f] Assumed equal to AOB.
[g] (Liu and Wang, 2014; Metcalf and Eddy, 2003).
[h] (Mehrani et al., 2021).
[i] (Yu et al., 2020).
[j] (Liu et al., 2020).
[k] (Henze et al., 2000).
[l] (Ni et al., 2011a; Samie et al., 2011).

two-step nitrification modeling studies (Table S1), and the initial biomass concentrations have not been even provided in some cases. In the present study, the result of model calibration revealed that the relative abundances of NOB were lower than those of AOB in both experimental trials (NOB/AOB ratios of 0.35 and 0.5). These ratios are generally in accordance with the previous two-step nitrification modeling studies (Table S1). In most of those studies, when the biomass concentrations are available, the initial NOB/AOB ratios ranged from 0.1 to 0.6 with the most common value of 0.2. For comparison, higher NOB/AOB ratios (0.8–1.5) have been reported for full-scale WWTPs (Harms et al., 2003; Ramdhani et al., 2014).

In theory, the ratio of NOB/AOB abundances in fully nitrifying systems should correspond to the ratio of their yield coefficients (Y_{NOB}/Y_{AOB}). When assuming the typical values from Metcalf and Eddy (2014), i.e. $Y_{NOB} = 0.05$ and $Y_{AOB} = 0.15$, the obtained ratio NOB/AOB = 0.33 suggests that AOB should dominate over NOB. In practice, however, the AOB and NOB abundances in nitrifying communities can shift and change depending on the local conditions (Cao et al., 2017). For example, Laureni et al. (2016) found significant differences in the NOB/AOB ratios, i.e. respectively 0.3 vs. 3.0 in the floc phase and biofilm, in a deammonification moving bed biofilm reactor. When the DO set point was reduced from 1.2 to <0.2 mgO_2/L. The NOB/AOB ratio fell to 0.04 in the floc phase, while it remained stable in the biofilm.

In contrast to the concentration of heterotrophic biomass, which can directly be estimated by three respirometric methods (Li et al., 2019), there are no such methods for nitrifiers. The nitrifier biomass concentration could be estimated in combination with kinetic parameters while fitting model predictions to experimental data (Chandran et al., 2008).

The systematic protocol, proposed in this study, is an advancement in comparison with previous studies. The traditional approaches to a preliminary estimation of the active AOB and NOB biomass concentration are based on the influent BOD/N ratio (Metcalf and Eddy, 1991) or mass balance equations, including the yields, amounts of substrate consumed, SRT and decay rates (Dold et al., 2005; Metcalf and Eddy, 2014). Model calibration has been a widely accepted method for estimation of the nitrifier biomass concentration in activated sludge systems, but the results depend on the applied model concept. For example, Hiatt and Grady (2008) found that the difference between one- and two-step models was approximately 20 % (39.7 vs. 47.6 mg COD/L). Other methods comprise microbiological analyses, such as fluorescence in situ hybridization (FISH), qPCR, more recently high-throughput 16S rRNA gene amplicon sequencing and metagenomics approach (Table S1).

The reported data on the dynamics of AOB and NOB abundances in WWTPs are ambiguous, even within a single plant. Based on stoichiometric calculations of influent COD, removal of total kjeldahl nitrogen (TKN) and adjusted kinetic parameters, Mota et al. (2005) found that the relative abundance of AOB remained relatively constant in different operational periods. In contrast, the relative abundance of AOB determined by FISH was significantly different throughout the periods. Moreover, under favourable conditions for nitrification (low C/N ratio and high ammonia in the influent), the nitrifier abundance reached 30 % (Mota et al., 2005).

Griffin and Wells (2017) reported more typical, up to 4 %, abundances of nitrifiers (*Nitrosomonas* and *Nitrobacter*) of the total microbial community in six municipal WWTPs. However, apart from one case, the *Nitrospira* abundance exhibited strong seasonal variabilities (0–3.5 %), whereas the *Nitrosomonas* abundance remained relatively stable (0.2–1.0 %). Johnston et al. (2019) found that the abundances of AOB and NOB remained relatively stable throughout the year. The authors found that the relative abundance of the overall nitrifier community, comprising known AOB and NOB, was approximately 1 %. However, the authors emphasized that this relative abundance was within the lower range of typical abundances for nitrifier communities in activated sludge systems. One of the principal reasons for these differences is that nitrification can be performed by unclassified groups of microorganisms. For example, Johnston et al. (2019) hypothesized that the abundant members of the heterotrophic family *Saprospiraceae* (approx. 8 % of the overall community in their study) could also be involved in nitrification.

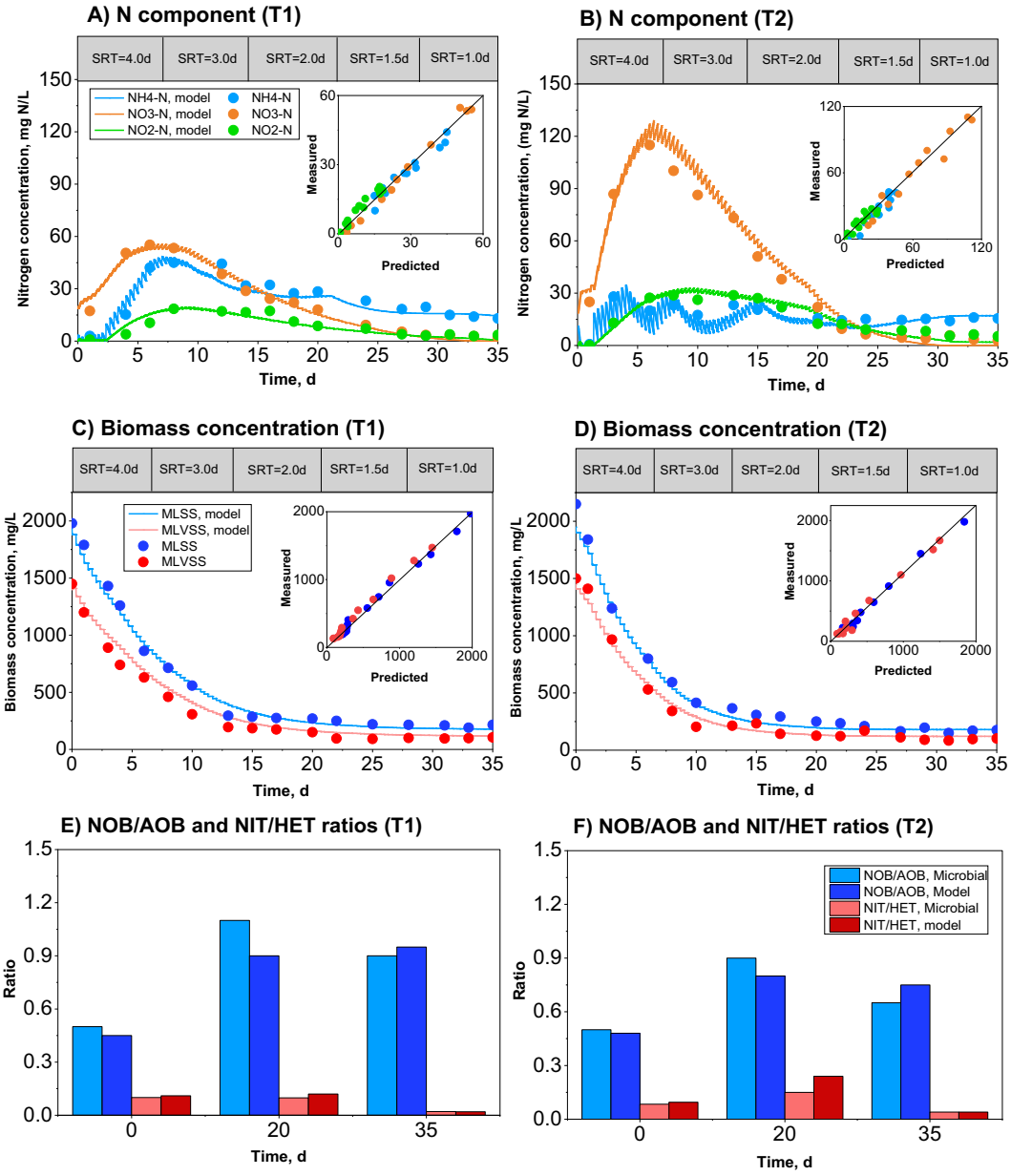

Fig. 4. Modeling and goodness-of-fit for the calibrated model in experiments T1 and T2 A) N components (T1), B) N components (T2), C) Biomass concentrations (T1), D) Biomass concentrations (T2), E) Ratios of NOB/AOB and NIT/HET (T1), F) Ratios of NOB/AOB and NIT/HET (T2).

Table 3
Summary of the model efficiency measures during the calibration and validation steps.

Step	Experiment	Output	R^2	RMSE	MAE	J^2
Calibration	T 1	NH_4^+-N	0.94	2.43	2.62	–
		NO_3^--N	0.93	3.38	2.50	–
		NO_2^--N	0.88	3.71	3.02	–
	T 2	NH_4^+-N	0.94	2.17	3.18	–
		NO_3^--N	0.91	2.3	2.91	–
		NO_2^--N	0.83	3.74	4.01	–
Validation	T 3	NH_4^+-N	0.85	3.24	3.87	1.61
		NO_3^--N	0.84	4.12	3.91	1.45
		NO_2^--N	0.81	4.78	4.18	1.62
	T 4	NH_4^+-N	0.84	3.11	4.22	2.05
		NO_3^--N	0.79	3.45	4.67	2.25
		NO_2^--N	0.74	4.75	5.45	1.6

4.2. The effect of comammox

In the present study, complete ammonia oxidation played a major role (18 %) at the beginning of the experiment, while in the middle phase and at the end, it had a minor role as a NH_4^+-N conversion pathway (2–5 %), which is in line with the results of a few earlier studies (Gonzalez-Martinez et al., 2016; Annavajhala et al., 2018). In contrast, the dominance of comammox bacteria over the other nitrifiers was observed in N removal systems under either DO-limited conditions (Roots et al., 2019; Wang et al., 2020; Sakoula et al., 2021). Therefore, comammox should not be ignored when modeling nitrification as a two-step process.

The low abundance of comammox bacteria, observed in this study, could be attributed to the process conditions unfavorable for "K-strategists", including extremely short SRTs and high ammonia loads. The dominance of comammox bacteria normally occurs at low nitrite concentrations with long SRTs (>40 d), coupled with low ammonia (<15 mg N/L) and low DO

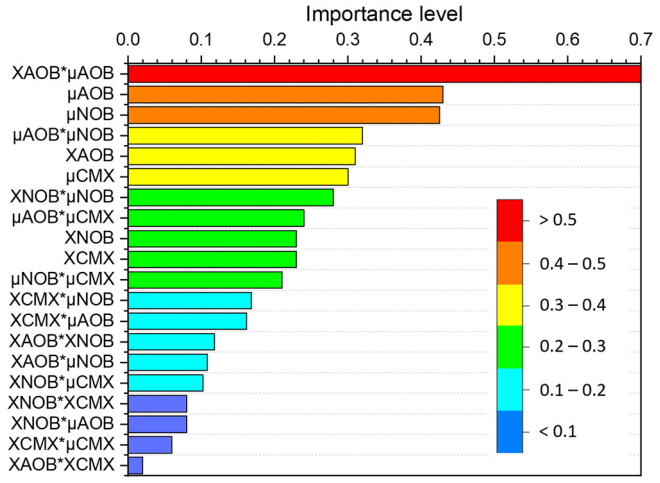

Fig. 5. Importance level of the inputs and their combinations (the top 20 influential inputs) on the calibration accuracy (RMSE for the sum of NH_4^+-N, NO_3^--N, and NO_2^--N).

conditions (<0.5 mg O_2/L) (Shao and Wu, 2021; Qian et al., 2017; Park et al., 2017; Wang et al., 2020).

In general, the mechanism of comammox is well established and involves sequential oxidation of ammonia to nitrate (NO_3^--N) via nitrite (NO_2^--N). Comammox *Nitrospira* possess genes relevant for both nitrification steps, i.e. ammonia monooxygenase (Amo) and hydroxylamine dehydrogenase (Hao) involved in ammonia oxidation, and nitrite oxidoreductase (Nxr) involved in nitrite oxidation (Daims et al., 2015; van Kessel et al., 2015). However, there is no consensus in literature whether (i) nitrite (NO_2^--N) is released outside of the cells during the comammox process, and (ii) comammox bacteria can grow using nitrite (NO_2^--N) as sole substrate. Those uncertainties led to the development of three possible conceptual models of comammox (Mehrani et al., 2021).

Despite different conceptual formulations of the comammox process, resulting in a high variability of μ_{CMX} (0.15–0.6 d^{-1}), the reliability and robustness of the models were similar in terms of predicting the N conversions. The lowest μ_{CMX} was obtained for the model concept used in the present study (one step oxidation of ammonia to nitrate). This value is only slightly lower compared to the present study (μ_{CMX} = 0.2 d^{-1}) run with biomass from a different WWTP. This may suggest that μ_{CMX} is relatively stable for a specific model concept.

Daims et al. (2016) hypothesized that low nitrite concentrations, observed in comammox systems, would result from processing nitrite inside the cells. Moreover, Wu et al. (2019) experimentally confirmed that NH_4^+-N was consumed by comammox, while NO_3^--N was simultaneously produced at a NO_3^--N/ NH_4^+-N ratio of nearly 1:1. Based on those results, the authors proposed a conceptual model of nitrogen removal by concurrent partial nitrification-anammox and one-step comammox. On the other hand, transient NO_2^--N accumulation produced by comammox *Nitrospira* during oxidation of NH_4^+-N was reported in several studies (Kits et al., 2017; Ren et al., 2020; Sakoula et al., 2021), as a result of the extracellular transit during complete nitrification.

Unlike canonical NOB, the currently known comammox *Nitrospira* cannot grow solely on NO_2^--N (Koch et al., 2019). The authors explained that inability by a low nitrite affinity of these bacteria based on the results of an earlier study of Kits et al. (2017). The nitrite affinity of canonical *Nitrospira* was approximately 50-fold higher in comparison with comammox *Nitrospira* (Kits et al., 2017). In a very recent study, Sakoula et al. (2021) showed that a novel comammox species was capable of nitrite oxidation. The estimated $K_{NO2,CMX}$ was below 0.2 mg N/L and remained in a lower range of K_{NO2} for different canonical NOB. In general, however, the data on kinetic and stoichiometric parameters for the comammox process are still very limited (Mehrani et al., 2021).

4.3. The effect of denitrifying heterotrophs grown on SMP

In the present study, heterotrophic denitrification was an important N conversion pathway. NO_3^--N reduction and increased from 5 % to 18.5 % in the course of the experiment. NO_2^--N reduction was more significant, especially at the end, when almost 50 % of N was converted via denitritation. These results are in contradiction with the commonly accepted approach for modeling nitrification that the effect of heterotrophic activity is neglected due to the lack of organic carbon in the feed.

In fact, the growth of heterotrophic bacteria has been observed in the systems fed only with inorganic substrates (Al-Hazmi et al., 2021; Liu et al., 2016; Lu et al., 2018; Ni et al., 2011b; Sepehri and Sarrafzadeh, 2019). The produced SMP could be the sole organic carbon and energy source for denitrifying heterotrophs (Ni et al., 2011b). Heterotrophic

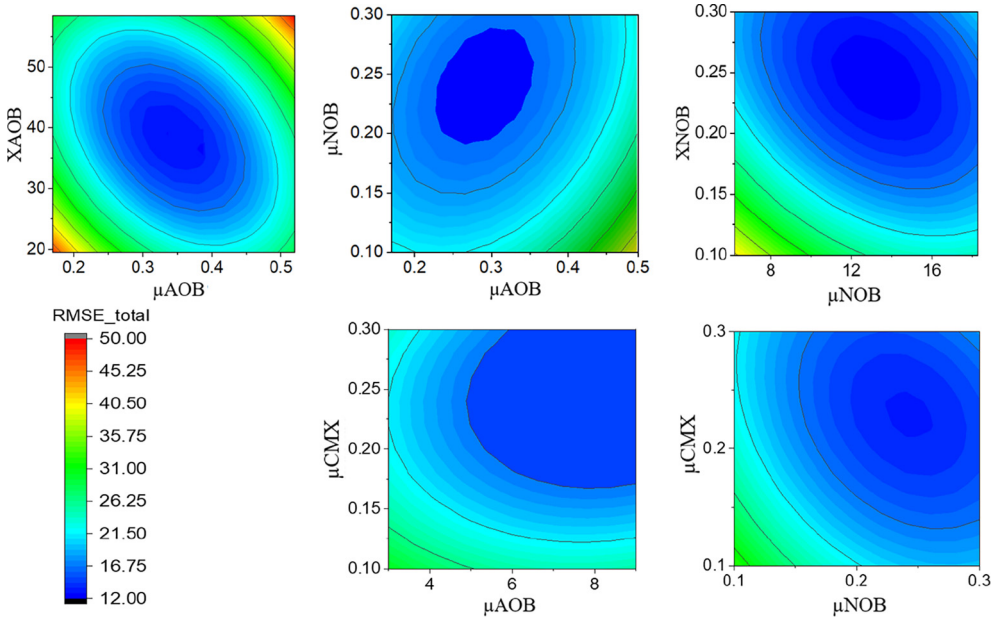

Fig. 6. Impact of the most important input parameters (initial biomass concentrations and maximum specific growth rates of nitrifiers) on the total RMSE (sum of NH_4^+-N, NO_3^--N, and NO_2^--N).

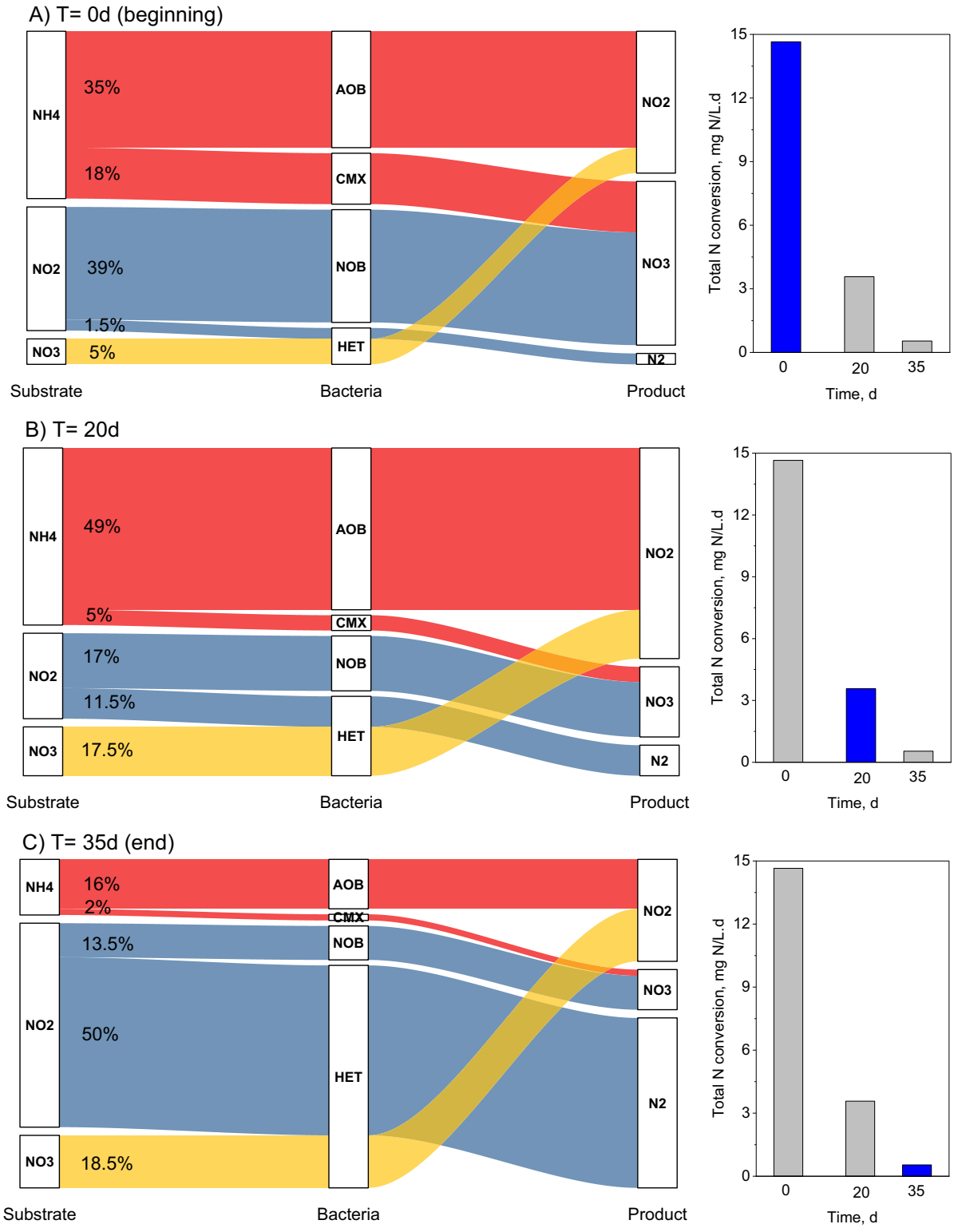

Fig. 7. Conversion pathways of the N species during experiment T1 (% represent the shares in the absolute total N conversions (mg N/L·d) shown on the right): A) 0 d, B) 20 d, C) 35 d.

bacteria can thrive on SMP and even low concentrations of SMP (25 mg COD/L) are expected to provide an energy and carbon source for denitrifying heterotrophs, while improving nitrogen removal rates and efficiencies (Zhang et al., 2016; Lackner et al., 2008).

Inorganic carbon is consumed in the growth of autotrophic nitrifying bacteria, and SMP are produced from the nitrifier biomass growth and decay (Liu et al., 2016). Normally, in activated sludge systems, this pathway is relatively insignificant. For example, Xie et al. (2012) found that nitrifiers contributed to SMP production in <8 %, including 5 and 3 % by the contributions of AOB and NOB, respectively. Sepehri and Sarrafzadeh (2019) observed that AOB produced more SMP (3 mg/L in total) than NOB (1.6 mg/L in total). The SRT had a strong effect on SMP production, and decreasing the SRT from 15 to 0.5 d resulted in the reduced SMP production by 62 % (Xie et al., 2012; Xie et al., 2016). In the present

study, the reduced SMP production at short SRTs did not limit the dominance of denitrifying heterotrophs in the microbial population towards the end of the trials.

Models describing formation and degradation of SMPs have been developed as either stand-alone models or more commonly ASM extensions (Makinia and Zaborowska, 2020). The use of ASM extensions with the SMP concepts was suggested when modeling (i) biology-based membrane fouling, (ii) soluble COD predictions, (iii) systems with long SRTs (Fenu et al., 2010). Sepehri and Sarrafzadeh (2019) proposed a conceptual model of interactions between nitrifiers and heterotrophs in a system fed with inorganic substrate. Liu et al. (2016) developed a theoretical model for the biological processes occurring in an anammox biofilm system (fed with no organic carbon). Organic carbon for the growth of the heterotrophic bacteria was exclusively derived from three internal sources: growth and decay of anammox and heterotrophic bacteria, and hydrolysis of EPS. Lu et al. (2018) expanded the ASM1 with the concept of Liu et al. (2016) to predict the heterotrophic growth in a deammonification system (fed with no organic carbon). The SMP were not only derived from the activity of anammox and heterotrophs, but also both groups of nitrifiers (AOB and NOB).

5. Conclusions

In this study, the ASM1 was extended to two-step nitrification, comammox and heterotrophic denitrification on SMP for removing nitrogen and organic matter. The model was successfully calibrated and validated with experimental data from an SBR nitrification process under different operational conditions, i.e., temperature (12 and 20 °C), aeration mode (continues and intermittent), and decreasing SRT from 4d to 1d. The following conclusions can be derived from this study:

- For identification of the relevant N pathways in nitrifying systems (especially under low DO conditions), two-step nitrification models should be extended with the accompanying processes, such as comammox and heterotrophic denitrification on SMP.
- Neglecting those processes may result in the substantial overestimation (>15 % in this study) of the maximum specific growth rates of AOB and NOB, despite similar prediction accuracies of the conventional and extended models in the long-term washout experiments.
- The combined effect of the initial biomass concentration of AOB and their maximum specific growth rate had the highest importance level for model calibration (0.7) based on the long-term behavior of N species. The individual effects of the maximum specific growth rates of nitrifiers (AOB, NOB, CMX) had higher importance levels (0.31–0.44) than the combined effect of the initial biomass concentration of NOB and their maximum specific growth rate (0.29).
- In the course of the experiments, the comammox share in the absolute total N conversions decreased from approximately 20 % to 2 %. Although comammox bacteria played a minor role, compared to the canonical nitrifiers, in the N conversions, the impact of that process should further be explored when modeling systems with higher abundances of *Nitrospira*.

CRediT authorship contribution statement

Mohamad-Javad Mehrani: Conceptualization, Data curation, Formal analysis, Methodology, Visualization, Investigation, Writing – original draft, Writing – review & editing. **Dominika Sobotka:** Data curation, Formal analysis, Investigation, Resources, Writing – review & editing. **Przemyslaw Kowal:** Data curation, Formal analysis, Investigation, Resources, Writing – review & editing. **Jianhua Guo:** Resources, Investigation, Writing – review & editing. **Jacek Mąkinia:** Conceptualization, Supervision, Funding acquisition, Project administration, Resources, Methodology, Formal analysis, Writing – original draft, Writing – review & editing.

Data availability

Data will be made available on request.

Declaration of competing interest

The authors declare that they have no known competing financial interests or personal relationships that could have appeared to influence the work reported in this paper.

Acknowledgments

This study was supported by the Polish National Science Center under project no. UMO-2017/27/B/NZ9/01039.

Appendix A. Supplementary data

Supplementary data to this article can be found online at https://doi.org/10.1016/j.scitotenv.2022.157628.

References

Al-Hazmi, H.E., Lu, X., Majtacz, J., Kowal, P., Xie, L., Makinia, J., 2021. Optimization of the aeration strategies in a deammonification sequencing batch reactor for efficient nitrogen removal and mitigation of N2O production. Environ. Sci. Technol. 55 (2), 1218–1230. https://doi.org/10.1021/acs.est.0c04229.

Annavajhala, M., Kapoor, V., Santo-Domingo, J., Chandran, K., 2018. Comammox functionality identified in diverse engineered biological wastewater treatment systems. Environ. Sci. Technol. Lett. 25, 110–116. https://doi.org/10.1021/acs.estlett.7b00577.

Anupam, K., Dutta, S., Bhattacharjee, C., Datta, S., 2011. Adsorptive removal of chromium (VI) from aqueous solution over powdered activated carbon: optimisation through response surface methodology. Chem. Eng. J. 173 (1), 135–143. https://doi.org/10.1016/j.cej.2011.07.049.

Baruah, J., Chaliha, C., Nath, B.K., Kalita, E., 2021. Enhancing arsenic sequestration on ameliorated waste molasses nanoadsorbents using response surface methodology and machine-learning frameworks. Environ. Sci. Pollut. Res. 28 (9), 11369–11383. https://doi.org/10.1007/s11356-020-11259-0.

Cao, J., Zhang, T., Wu, Y., Sun, Y., Zhang, Y., Huang, B., Fu, B., Yang, E., Zhang, Q., Luo, J., 2020. Correlations of nitrogen removal and core functional genera in full-scale wastewater treatment plants: influences of different treatment processes and influent characteristics. Bioresour. Technol. 297, 122455. https://doi.org/10.1016/j.biortech.2019.122455.

Cao, Y., van Loosdrecht, M.C.M., Daigger, G.T., 2017. Mainstream partial nitritation–anammox in municipal wastewater treatment: status, bottlenecks, and further studies. Appl. Microbiol. Biotechnol. 101 (4), 1365–1383. https://doi.org/10.1007/s00253-016-8058-7.

Chandran, K., Hu, Z., Smets, B.F., 2008. A critical comparison of extant batch respirometric and substrate depletion assays for estimation of nitrification biokinetics. Biotechnol. Bioeng. 101, 62–72.

Metcalf and Eddy, Inc., 2014. Wastewater Engineering: Treatment and Resource Recovery. 5th edition. McGraw-Hill, New York, United States.

Daims, H., Lebedeva, E.V., Pjevac, P., Han, P., Herbold, C., Albertsen, M., Jehmlich, N., Palatinszky, M., Vierheilig, J., Bulaev, A., Kirkegaard, R.H., von Bergen, M., Rattei, T., Bendinger, B., Nielsen, P.H., Wagner, M., 2015. Complete nitrification by Nitrospira bacteria. Nature 528 (7583), 504–509. https://doi.org/10.1038/nature16461.

Daims, H., Lücker, S., Wagner, M., 2016. A new perspective on microbes formerly known as nitrite-oxidizing bacteria. Trends Microbiol. 24 (9), 699–712. https://doi.org/10.1016/j.tim.2016.05.004.

Dold, P.L., Jones, R.M., Bye, C.M., 2005. Importance and measurement of decay rate when assessing nitrification kinetics. Water Sci. Technol. 52 (10–11), 469–477. https://doi.org/10.2166/wst.2005.0725.

Fenu, A., Guglielmi, G., Jimenez, J., Spèrandio, M., Saroj, D., Lesjean, B., Brepols, C., Thoeye, C., Nopens, I., 2010. Activated sludge model (ASM) based modelling of membrane bioreactor (MBR) processes: a critical review with special regard to MBR specificities. Water Res. 44 (15), 4272–4294. https://doi.org/10.1016/j.watres.2010.06.007.

Gilbert, E.M., Agrawal, S., Karst, S.M., Horn, H., Nielsen, P.H., Lackner, S., 2014. Low temperature partial nitritation/anammox in a moving bed biofilm reactor treating low strength wastewater. Environ. Sci. Technol. 48 (15), 8784–8792. https://doi.org/10.1021/es501649m.

Gonzalez-Martinez, A., Rodriguez-Sanchez, A., van Loosdrecht, M.C.M., et al., 2016. Detection of comammox bacteria in full-scale wastewater treatment bioreactors using *tag*-454-pyrosequencing. Environ. Sci. Pollut. Res. 23. https://doi.org/10.1007/s11356-016-7914-4.

Griffin, J., Wells, G., 2017. Regional synchrony in full-scale activated sludge bioreactors due to deterministic microbial community assembly. ISMG 11. https://doi.org/10.1038/ismej.2016.121.

Gustavsson, D.J.I., Suarez, C., Wilén, B.-M., Hermansson, M., Persson, F., 2020. Long-term stability of partial nitritation-anammox for treatment of municipal wastewater in a moving bed biofilm reactor pilot system. Sci. Total Environ. 714, 136342.

Harms, G., Layton, A.C., Dionisi, H.M., et al., 2003. Real-time PCR quantification of nitrifying bacteria in a municipal wastewater treatment plant. Environ. Sci. Technol. 37, 343–351. https://doi.org/10.1021/es0257164.

Hauduc, H., Neumann, M.B., Muschalla, D., Gamerith, V., Gillot, S., Vanrolleghem, P.A., 2015. Efficiency criteria for environmental model quality assessment: a review and its application to wastewater treatment. Environ. Model Softw. 68, 196–204. https://doi.org/10.1016/j.envsoft.2015.02.004.

Henze, M.G.W., Mino, T., van Loosdrecht, M.C.M., 2000. Activated Sludge Models ASM1, ASM2, ASM2d and ASM3. IWA Publishing, London, UK.
Hiatt, W.C., Grady, C.P.L., 2008. An updated process model for carbon oxidation, nitrification, and denitrification. Water Environ. Res. 80 (11), 2145–2156. https://doi.org/10.2175/106143008X304776.
Johnston, J., LaPara, T., Behrens, S., 2019. Composition and dynamics of the activated sludge microbiome during seasonal nitrification failure. Sci. Rep. 9 (1), 4565. https://doi.org/10.1038/s41598-019-40872-4.
Kaelin, D., Manser, R., Rieger, L., Eugster, J., Rottermann, K., Siegrist, H., 2009. Extension of ASM3 for two-step nitrification and denitrification and its calibration and validation with batch tests and pilot scale data. Water Res. 43 (6), 1680–1692. https://doi.org/10.1016/j.watres.2008.12.039.
Kits, A., Sedlacek, C., Lebedeva, E., et al., 2017. Kinetic analysis of a complete nitrifier reveals an oligotrophic lifestyle. Nature 549, 269–272. https://doi.org/10.1038/nature23679.
Knowles, G., Downing, A.L., Barrett, M.J., 1965. Determination of kinetic constants for nitrifying bacteria in mixed culture, with the aid of an electronic computer. Microbiology 38 (2), 263–278. https://doi.org/10.1099/00221287-38-2-263.
Koch, H., Lücker, S., van Kessel, 2019. Complete nitrification: insights into the ecophysiology of comammox Nitrospira. Appl. Microbiol. Biotechnol. 103 (1), 177–189. https://doi.org/10.1007/s00253-018-9486-3.
Lackner, S., Terada, A., Smets, B.F., 2008. Heterotrophic activity compromises autotrophic nitrogen removal in membrane-aerated biofilms: results of a modeling study. Water Res. 42 (4), 1102–1112. https://doi.org/10.1016/j.watres.2007.08.025.
Laureni, M., Falås, P., Robin, O., Wick, A., Weissbrodt, D.G., Nielsen, J.L., Ternes, T.A., Morgenroth, E., Joss, A., 2016. Mainstream partial nitritation and anammox: long-term process stability and effluent quality at low temperatures. Water Res. 101, 628–639. https://doi.org/10.1016/j.watres.2016.05.005.
Li, B., Gan, L., Owens, G., Chen, Z., 2018. New nano-biomaterials for the removal of malachite green from aqueous solution via a response surface methodology. Water Res. 146, 55–66. https://doi.org/10.1016/j.watres.2018.09.006.
Li, Z.-H., Hang, Z.-Y., Lu, M., Zhang, T.-Y., Yu, H.-Q., 2019. Difference of respiration-based approaches for quantifying heterotrophic biomass in activated sludge of biological wastewater treatment plants. Sci. Total Environ. 664, 45–52. https://doi.org/10.1016/j.scitotenv.2019.02.007.
Liu, G., Wang, J., 2014. Role of solids retention time on complete nitrification: mechanistic understanding and modeling. J. Environ. Eng. 48. https://doi.org/10.1061/(ASCE)EE.1943-7870.0000779.
Liu, X., Kim, M., Nakhla, G., Andalib, M., Fang, Y., 2020. Partial nitrification-reactor configurations, and operational conditions: performance analysis. J. Environ. Chem. Eng. 8 (4), 103984. https://doi.org/10.1016/j.jece.2020.103984.
Liu, Y., Sun, J., Peng, L., Wang, D., Dai, X., Ni, B.-J., 2016. Assessment of heterotrophic growth supported by soluble microbial products in anammox biofilm using multidimensional modeling. Sci. Rep. 6 (1), 27576. https://doi.org/10.1038/srep27576.
Liu, Y., Li, S., Ni, G., Duan, H., Huang, X., Yuan, Z., Zheng, M., 2021. Temperature variations shape niche occupation of nitrotoga-like bacteria in activated sludge. ACS ES&T Water 1 (1), 167–174. https://doi.org/10.1021/acsestwater.0c00060.
Lu, X., Pereira, D.S., Al-Hazmi, T.H.E., Majtacz, J., Zhou, Q., Xie, L., Makinia, J., 2018. Model-based evaluation of N2O production pathways in the anammox-enriched granular sludge cultivated in a sequencing batch reactor. Environ. Sci. Technol. 52 (5), 2800–2809. https://doi.org/10.1021/acs.est.7b05611.
Makinia, J., Zaborowska, E., 2020. Mathematical Modelling and Computer Simulation of Activated Sludge Systems. IWA, UK.
Mehrani, M.-J., Lu, X., Kowal, P., Sobotka, D., Mąkinia, J., 2021. Incorporation of the complete ammonia oxidation (comammox) process for modeling nitrification in suspended growth wastewater treatment systems. J. Environ. Manag. 297, 113223. https://doi.org/10.1016/j.jenvman.2021.113223.
Metcalf and Eddy, Inc., 1991. Wastewater Engineering: Treatment, Disposal, and Reuse. 3rd edition. McGraw-Hill, New York, United States.
Metcalf and Eddy, Inc., 2003. Wastewater Engineering: Treatment and Reuse. 4th edition. McGraw-Hill, New York, United States.
Mota, C., Ridenoure, J., Cheng, J., de los Reyes III, F.L., 2005. High levels of nitrifying bacteria in intermittently aerated reactors treating high ammonia wastewater. FEMS Microbiol. Ecol. 54 (3), 391–400. https://doi.org/10.1016/j.femsec.2005.05.001.
Mozumder, M.S.I., Picioreanu, C., van Loosdrecht, M.C.M., Volcke, E.I.P., 2014. Effect of heterotrophic growth on autotrophic nitrogen removal in a granular sludge reactor. Environ. Technol. 35 (8), 1027–1037. https://doi.org/10.1080/09593330.2013.859711.
Ni, B.-J., Ruscalleda, M., Pellicer-Nàcher, C., Smets, B.F., 2011a. Modeling nitrous oxide production during biological nitrogen removal via nitrification and denitrification: extensions to the general ASM models. Environ. Sci. Technol. 45 (18), 7768–7776. https://doi.org/10.1021/es201489n.
Ni, B.-J., Xie, W.-M., Chen, Y.-P., Fang, F., Liu, S.-Y., Ren, T.-T., Sheng, G.-P., Yu, H.-Q., Liu, G., Tian, Y.-C., 2011b. Heterotrophs grown on the soluble microbial products (SMP) released by autotrophs are responsible for the nitrogen loss in nitrifying granular sludge. Biotechnol. Bioeng. 108 (12), 2844–2852. https://doi.org/10.1002/bit.23247.
Park, M.-R., Park, H., Chandran, K., 2017. Molecular and kinetic characterization of planktonic Nitrospira spp. selectively enriched from activated sludge. Environ. Sci. Technol. 51 (5), 2720–2728. https://doi.org/10.1021/acs.est.6b05184.
Pjevac, P., Schauberger, C., Poghosyan, L., Herbold, C.W., van Kessel, M.A.H.J., Daebeler, A., Steinberger, M., Jetten, M.S.M., Lücker, S., Wagner, M., et al., 2017. AmoA-targeted polymerase chain reaction primers for the specific detection and quantification of comammox nitrospira in the environment. Front. Microbiol. 8, 1508. https://doi.org/10.3389/fmicb.2017.01508.
Qian, F., Wang, J., Shen, Y., et al., 2017. Achieving high performance completely autotrophic nitrogen removal in a continuous granular sludge reactor. Biochem. Eng. J. 15, 97–104. https://doi.org/10.1016/j.bej.2016.11.017.
Ramdhani, N., Kumari, S., Bux, F., 2014. Distribution of Nitrosomonas-related ammonia-oxidizing bacteria and Nitrobacter-related nitrite-oxidizing bacteria in two full-scale biological nutrient removal plants. Water Environ. Res. https://doi.org/10.2175/106143013x13596524516022. PMID: 23697242.
Regmi, P., Miller, M.W., Holgate, B., Bunce, R., Park, H., Chandran, K., Wett, B., Murthy, S., Bott, C.B., 2014. Control of aeration, aerobic SRT and COD input for mainstream nitritation/denitritation. Water Res. 57, 162–171. https://doi.org/10.1016/j.watres.2014.03.035.
Ren, Y., Ngo, H.H., Guo, W., et al., 2020. New perspectives on microbial communities and biological nitrogen removal processes in wastewater treatment systems. Bioresour. Technol. 297, 122491. https://doi.org/10.1016/j.biortech.2019.122491.
Roots, P., Wang, Y., Rosenthal, A.F., et al., 2019. Comammox nitrospira are the dominant ammonia oxidizers in a mainstream low dissolved oxygen nitrification reactor. Water Res. 175, 396–405. https://doi.org/10.1016/j.watres.2019.03.060.
Sakoula, D., Koch, H., Frank, J., 2021. Enrichment and physiological characterization of a novel comammox nitrospira indicates ammonium inhibition of complete nitrification. ISME J. 15, 1010–1024. https://doi.org/10.1038/s41396-020-00827-4.
Samie, G., Bernier, J., Rocher, V., Lessard, P., 2011. Modeling nitrogen removal for a denitrification biofilter. Bioprocess Biosyst. Eng. 34 (6), 747–755. https://doi.org/10.1007/s00449-011-0524-0.
Sepehri, A., Sarrafzadeh, M.-H., 2019. Activity enhancement of ammonia-oxidizing bacteria and nitrite-oxidizing bacteria in activated sludge process: metabolite reduction and CO2 mitigation intensification process. Appl. Water Sci. 9 (5), 131. https://doi.org/10.1007/s13201-019-1017-6.
Shao, Y.-H., Wu, J.-H., 2021. Comammox nitrospira species dominate in an efficient partial nitrification-anammox bioreactor for treating ammonium at low loadings. Environ. Sci. Technol. 55 (3), 2087–2098. https://doi.org/10.1021/acs.est.0c05777.
van Kessel, M.A.H.J., Speth, D.R., Albertsen, M., Nielsen, P.H., Op den Camp, H.J.M., Kartal, B., Jetten, Lücker, S., 2015. Complete nitrification by a single microorganism. Nature 528, 555. https://doi.org/10.1038/nature16459.
Wang, Z., Zhang, L., Zhang, F., 2020. Nitrite accumulation in comammox-dominated nitrification-denitrification reactors: effects of DO concentration and hydroxylamine addition. J. Hazard. Mater. 15, 121375. https://doi.org/10.1016/j.jhazmat.2019.121375.
Wu, L., Shen, M., Li, J., et al., 2019. Cooperation between partial-nitrification, complete ammonia oxidation (comammox), and anaerobic ammonia oxidation (anammox) in sludge digestion liquid for nitrogen removal. Environ. Pollut. 254. https://doi.org/10.1016/j.envpol.2019.112965.
Xie, W.-M., Ni, B.-J., Seviour, T., Sheng, G.-P., Yu, H.-Q., 2012. Characterization of autotrophic and heterotrophic soluble microbial product (SMP) fractions from activated sludge. Water Res. 46 (19), 6210–6217. https://doi.org/10.1016/j.watres.2012.02.046.
Xie, W.-M., Ni, B.-J., Sheng, G.-P., Seviour, T., Yu, H.-Q., 2016. Quantification and kinetic characterization of soluble microbial products from municipal wastewater treatment plants. Water Res. 88 (1), 703–710.
Yin, Q., Sun, Y., Li, B., Feng, Z., Wu, G., 2022. The r/K selection theory and its application in biological wastewater treatment processes. Sci. Total Environ. 824, 153836. https://doi.org/10.1016/j.scitotenv.2022.153836.
Yu, L., Chen, S., Chen, W., Wu, J., 2020. Experimental investigation and mathematical modeling of the competition among the fast-growing "r-strategists" and the slow-growing "K-strategists" ammonium-oxidizing bacteria and nitrite-oxidizing bacteria in nitrification. Sci. Total Environ. 702, 135049. https://doi.org/10.1016/j.scitotenv.2019.135049.
Zhang, Y., Ma, H., Niu, Q., Chen, R., Hojo, T., Li, Y.-Y., 2016. Effects of soluble microbial products (SMP) on the performance of an anammox attached film expanded bed (AAFEB) reactor: synergistic interaction and toxic shock. Bioresour. Technol. 222, 261–269. https://doi.org/10.1016/j.biortech.2016.09.129.
Zhu, A., Guo, J., Ni, B.-J., Wang, S., Yang, Q., Peng, Y., 2015. A novel protocol for model calibration in biological wastewater treatment. Sci. Rep. 5 (1), 8493. https://doi.org/10.1038/srep08493.